Heliyon 10 (2024) e31202

Contents lists available at ScienceDirect

Heliyon

journal homepage: www.cell.com/heliyon

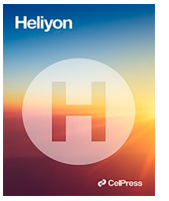

Research article

An anoikis-related lncRNA signature may predict the prognosis, immune infiltration, and drug sensitivity in esophageal cancer

Fan Feng, Yuxin Chu, Yi Yao, Bin Xu, Qibin Song *

Cancer Center, Renmin Hospital of Wuhan University, Wuhan, Hubei, 430060, PR China

ARTICLE INFO

Keywords:
Esophageal cancer
lncRNA
Anoikis
Survival

ABSTRACT

Background: Esophageal cancer (EC) is a prevalent malignancy with heterogeneous outcomes. This study explores the significance of anoikis-related long non-coding RNAs (lncRNAs) in EC, aiming to unravel their molecular roles and clinical implications.

Methods: Transcriptome and clinical data were obtained from TCGA database for EC samples. We identified anoikis-related genes and lncRNAs by Pearson correlation analysis. The risk score model hinged on prognostic lncRNAs filtered from multiple steps. Risk scores were calculated using the derived formula, and categorized patients into low- and high-risk groups. Model robustness was assessed through Kaplan-Meier (KM) survival analysis and Receiver Operating Characteristic (ROC) curve, with clinical utility achieved via a constructed nomogram. We also explored the interplay between the risk score and immune cell infiltration, and investigated drug sensitivity.

Results: We identified 2365 anoikis-related lncRNAs through co-expression analysis, including 1415 significant lncRNAs differentially expressed between normal and tumor samples. A risk score model was constructed from ten prognostic lncRNAs. The risk score model effectively stratified patients based on the median score, and its predictive capacity was validated through KM survival, ROC curve analyses, and the external GSE53622 dataset. The nomogram provided a practical tool for individualized prognosis evaluation. We unveiled significant correlations between specific immune cell subsets and the risk score. Eosinophils and common lymphoid progenitors exhibited positive associations, while endothelial cells and myeloid dendritic cells showed negative correlations. Drug sensitivity analysis revealed potential sensitive drugs for EC treatment that aligned with the risk subgroups.

Conclusion: This study established an anoikis-related lncRNAs risk score model that may predict the prognosis, immune infiltration, and drug sensitivity in EC, in hope of facilitating tailored patient management.

1. Introduction

Esophageal cancer (EC) remains a significant global health challenge due to its high incidence, poor prognosis, and limited treatment options [1]. In the year 2018 alone, EC accounted for a staggering 570,000 newly diagnosed cases and over 500,000 deaths, positioning it as the 7th most prevalent and the 6th most fatal cancer globally [2]. These concerning statistics underscore the urgent

* Corresponding author. Cancer Center, Renmin Hospital of Wuhan University, Jiefang Road No. 238, Wuhan, Hubei, 430060, PR China.
E-mail address: qibinsong@whu.edu.cn (Q. Song).

https://doi.org/10.1016/j.heliyon.2024.e31202
Received 28 November 2023; Received in revised form 7 May 2024; Accepted 13 May 2024
Available online 14 May 2024
2405-8440/© 2024 Published by Elsevier Ltd. This is an open access article under the CC BY-NC-ND license (http://creativecommons.org/licenses/by-nc-nd/4.0/).

need of innovative approaches to address the substantial impact of EC on human health. The integration of high-throughput molecular data and bioinformatic approaches has revolutionized cancer research, enabling the identification of predictive biomarkers that hold the prospect to improve prognosis evaluation, therapeutic strategies, and patient outcomes [3]. Among these emerging biomarkers, long non-coding RNAs (lncRNAs) have garnered considerable attention due to their regulatory roles in diverse biological processes and their potential as versatile indicators of cancer dynamics [4].

Anoikis, the process of programmed cell death triggered by loss of contact with the extracellular matrix, has been implicated in cancer metastasis and progression [5]. Aberrations in the anoikis pathway can profoundly influence tumor behavior, raising the prospect of exploiting anoikis-related molecular signatures as predictive tools [6]. In the context of EC, where effective prognostication and targeted therapy are pivotal [7], understanding the interplay between anoikis-related lncRNAs and disease prognosis holds significant clinical promise [8]. In response to this imperative, our study endeavors to investigate the predictive potential of an anoikis-related lncRNA signature in EC.

Based on the molecular and clinical data from the Cancer Genome Atlas (TCGA) platform, our analysis unfolds through multiple dimensions. It encompasses the identification of prognostic anoikis-related lncRNAs, the construction of a risk score model, and the evaluation of its prognostic performance. Moreover, we delve into the relationships between the risk score and immune cell infiltration, drug sensitivity, shedding light on potential avenues for personalized therapy. The integration of cutting-edge bioinformatics with clinical relevance underscores the transformative potential of our investigation [9]. By unraveling the molecular landscape of EC through the lens of an anoikis-related lncRNA signature, we aspire to bridge the gap between fundamental research and actionable clinical implications. Ultimately, this study may contribute to the expanding knowledge of lncRNA-mediated signatures in cancer, striving to translate the findings into improved prognostication, immune modulation, and treatment strategies for the EC patients.

2. Materials and methods

2.1. Data source and processing

We procured the transcriptome and clinical data for our study from the Cancer Genome Atlas (TCGA) database, accessible at https://portal.gdc.cancer.gov/. This comprehensive database encompassed RNA-seq profiles of individuals afflicted with esophageal carcinoma (ESCA). The quantification of gene expression levels was evaluated by the Fragments Per Kilobase of transcript per Million mapped reads (FPKM) value. The dataset consisted of 183 tumor samples from the esophageal squamous cell carcinoma (ESCC) patients, representing the diseased cohort, along with 13 matched normal tissue samples, which served as the control group. To ensure the ethical integrity of our study, all data used were derived from publicly available sources and had received the requisite approvals from the respective Ethics Committees. Notably, written informed consents from the patients were not required, given the de-identified and public nature of the dataset.

2.2. Identify anoikis-related genes and lncRNAs

We identified a set of 338 genes associated with anoikis from a previously publication (Supplementary Table S1) [10]. The anoikis-related gene (ARG) expression matrix was extracted by Perl scripts. The Perl scripts processed mRNA expression data by averaging replicates, filtering genes based on expression levels, and extracting a specified subset of genes associated with anoikis. It output the expression data for further analysis. Then we identified the anoikis-related lncRNAs by Pearson correlation analysis with the gene expression data. In light of the threshold of $|\text{correlation coefficient}| > 0.4$ and $P < 0.001$, we collected the significant anoikis-related lncRNAs for subsequent analysis. A correlation coefficient value of 0.4 was chosen to ensure that only correlations with a moderate to strong relationship are considered. The P-value of <0.001 indicated a high level of statistical significance, minimizing the probability of a Type I error. This threshold ensures that the identified lncRNAs have both a reasonably strong relationship with anoikis-genes and a robust statistical significance. Subsequently, a comparative assessment of lncRNA expression profiles between normal and tumor tissues was undertaken by the "limma" and relevant R packages.

2.3. Construct the risk score model

Based on the expression matrix of anoikis-related lncRNAs and survival data of the EC patients, we established a risk score model. First, we selected the lncRNAs significantly associated with patients' prognosis by univariate Cox regression analysis. Second, we further refined the prognostic anoikis-related lncRNAs by the Least Absolute Shrinkage and Selection Operator (LASSO) Cox analysis. Third, we identified the prognostic lncRNAs by multivariate Cox regression analysis. The criterion for significance in each step was $p < 0.05$. At length, 10 prognostic lnRNAs were collected. The coefficients for constructing risk score model were derived from multivariate Cox regression analysis for significant lnRNAs. This step identified the specific coefficients for each lncRNA, forming the basis of risk score formula. The risk score for an individual patient was calculated as the sum of the expression value of each selected lncRNA multiplied by its corresponding coefficient: risk score = Σ [coef(lncRNA) $\times$ Expr(lncRNA)]. In light of the coefficient and expression value of each lncRNA in our study, risk score = -0.825*$EMSLR$ + 1.098*$AC005013.1$ + 0.394*$AP002478.1$ + 0.392*$CASC8$ + 0.456*$AC025166.1$ + 2.171*$ZFAS1$ + 0.815*$AL355607.2$ + 1.865*$LINC02128$ + -1.704*$AC004817.5$ + 1.666*$AC051619.4$. Based on the calculated risk scores, the EC patients were categorized into low- and high-risk groups using the median value as the threshold. The median value was chosen as the cut-off due to its statistical property of being less influenced by outliers than mean values. This approach ensures a balanced division of the patient cohort, which helps to evaluate the prognostic utility of the risk score. Any given

patient's tumor sample, once assayed for the expression of these 10 lncRNAs and processed through the risk score formula, can be directly compared to the median risk score. Consequently, this helps to determine whether the patient falls into the low-risk or high-risk category, facilitating personalized prognosis evaluation and potential therapy customization.

2.4. Risk score model evaluation

The clinical utility and robustness of the constructed risk score model were evaluated. Kaplan-Meier (KM) survival analysis was conducted to assess the divergence in overall survival (OS) between the two risk groups. Receiver Operating Characteristic (ROC) curve analysis was employed to quantify the discriminatory power and accuracy of the risk score model. The area under the ROC curve (AUC) was calculated as a quantitative measure of the model's predictive performance. Moreover, this risk score model was validated by the external GSE53622 dataset from Gene Expression Omnibus (GEO) database. A nomogram was constructed to facilitate the clinical application of the risk score model. Nomogram is a graphical representation that combines all prognostic factors, including risk scores and relevant clinical features, into a single model. Each variable is assigned a value on a scale, typically from 0 to 100, based on its prognostic weight. These values are summed to provide a total score which correlates with a specific outcome, such as survival probability. By applying this tool to the individual patient's data, we enable clinicians to visualize and quantify the patient's predicted survival probability directly, thus enhancing clinical decision-making.

2.5. Relationship between risk score and immune cell infiltration

To unravel the interplay between risk score and the tumor immune microenvironment, we conducted an in-depth analysis of immune cell infiltration in EC. To gain an insight into the immune cell composition, we harnessed a suite of established computational tools, including TIMER, XCELL, QUANTISEQ, MCPCOUNTER, EPIC, CIBERSORTABS, and the CIBERSORT R script [11]. We employed several computational tools to quantitatively assess the presence of immune cell types within the tumor microenvironment. To reconcile the results from these tools, we adopted a multi-step process. Initially, each tool was independently used to estimate the immune cell composition from the gene expression data. Then, we performed a cross-validation step where the estimates from all tools were compared for consistency and correlative patterns. Subsequently, an integrated analysis was conducted using a consensus approach. By integrating these tools, we characterized the immune cell subsets and explored their correlations with the risk score model.

2.6. Drug sensitivity analysis

We conducted drug sensitivity analysis using the "oncoPredict" R package, which can identify drugs with sensitivity towards different risk subgroups [12]. By calculating the half-maximal inhibitory concentration (IC50) values of small molecular drugs, we sought to identify sensitive drugs for EC treatment that align with our risk score model. The "oncoPredict" R package was chosen for its robustness in integrating gene expression profiles with drug sensitivity data to predict therapeutic responses. Its comprehensive database of IC50 values for numerous drugs allows for a precise estimation of drug sensitivity. We used IC50 values as they are a standard measure of drug potency, with lower values indicating higher sensitivity of EC cells to the drugs. By correlating these values with our risk score model, we were able to delineate drugs that show increased effectiveness in different subgroups, potentially guiding tailored treatment strategies.

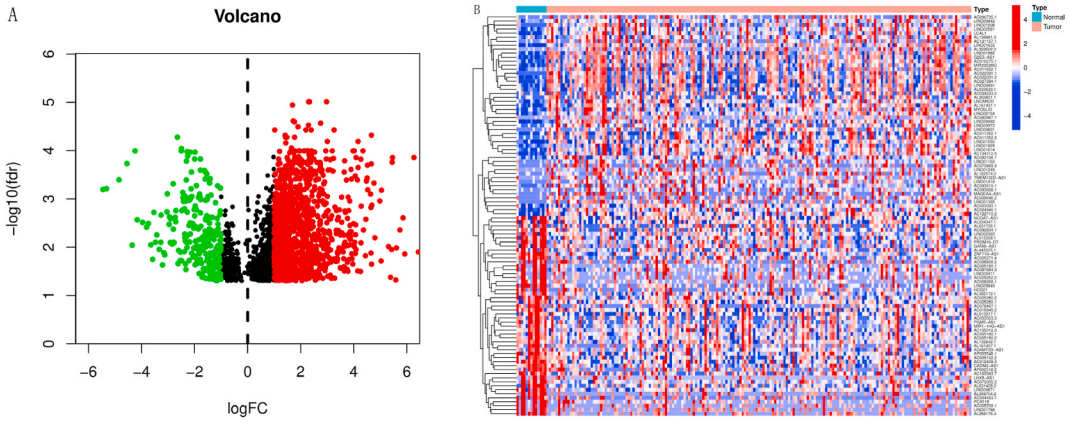

Fig. 1. The anoikis-related lncRNA expression pattern in esophageal cancer. (A) Volcano plot of the differentially expressed lncRNAs. (B) Heatmap of the lncRNA expression in normal and tumor samples.

2.7. Statistical analysis

Gene expression disparities between the two groups were examined using the Mann-Whitney *U* test. To gauge survival discrepancies among subgroups, we used Kaplan-Meier method with log-rank test. Correlation analysis entailed the Pearson and Spearman correlation test. A multivariate Cox regression model was employed to calculate the coefficients of prognostic lncRNAs, contributing to the construction of a risk score model. All the analyses were performed on R software (version 4.3.2). Across all tests, we deemed statistical significance when the p-value was <0.05.

3. Results

3.1. Anoikis-related lncRNA expression in EC

Through co-expression analysis, a collection of 2365 anoikis-related lncRNAs was retrieved. Subsequently, the differentially expressed lncRNAs between normal and tumor tissues was identified. For multiple testing adjustments, we considered the fold change (FC) and false discovery rate (FDR) in differential analysis. Employing the criteria ($|\text{Log2FC}| > 1$ and FDR <0.05), we obtained 1415 differential lncRNAs (Supplementary Table S2), including 1169 upregulated and 246 downregulated lncRNAs (Fig. 1A). The top 100 differential lncRNAs are visualized in the heat map (Fig. 1B).

3.2. Construct the anoikis-related lncRNAs risk score model

The anoikis-related lncRNA expression matrix was merged with the survival data of EC patients by matching TCGA sample ID. These lncRNAs were filtered by univariate Cox regression, LASSO-Cox, and multivariate Cox regression analysis. First, we obtained 59 anoikis-related lncRNAs from univariate Cox regression filter (Fig. 2A). The expression profile of these lncRNAs was also illustrated in a heat map (Fig. 2B).

Second, these prognostic lncRNAs were further filtered by LASSO-Cox regression analysis. We acquired 14 lncRNAs based on the penalty parameter lambda at the lowest partial likelihood deviance ($\lambda = 0.091$). LASSO-Cox regression analysis can identify the minimum deviance and optimal parameters of prognostic anoikis-related lncRNAs (Fig. 3A and B).

Third, the LASSO-significant anoikis-related lncRNAs were further filtered by multivariate Cox regression analysis. At length, we identified 10 prognostic lncRNAs, including *EMSLR, AC005013.1, AP002478.1, CASC8, AC025166.1, ZFAS1, AL355607.2, LINC02128, AC004817.5, AC051619.4*, for constructing the risk score model. To illustrate the flow of lncRNAs filtering process, we have made a Venn plot (Supplementary Fig. S1). The risk score of each sample was calculated according to the formula in method part. In light of the median risk score, the EC patients were dichotomized into the low-risk and high-risk groups.

3.3. Assess the risk score model

To assess the prognostic value of our risk score model in EC patients, KM survival analysis was used to compare the OS difference

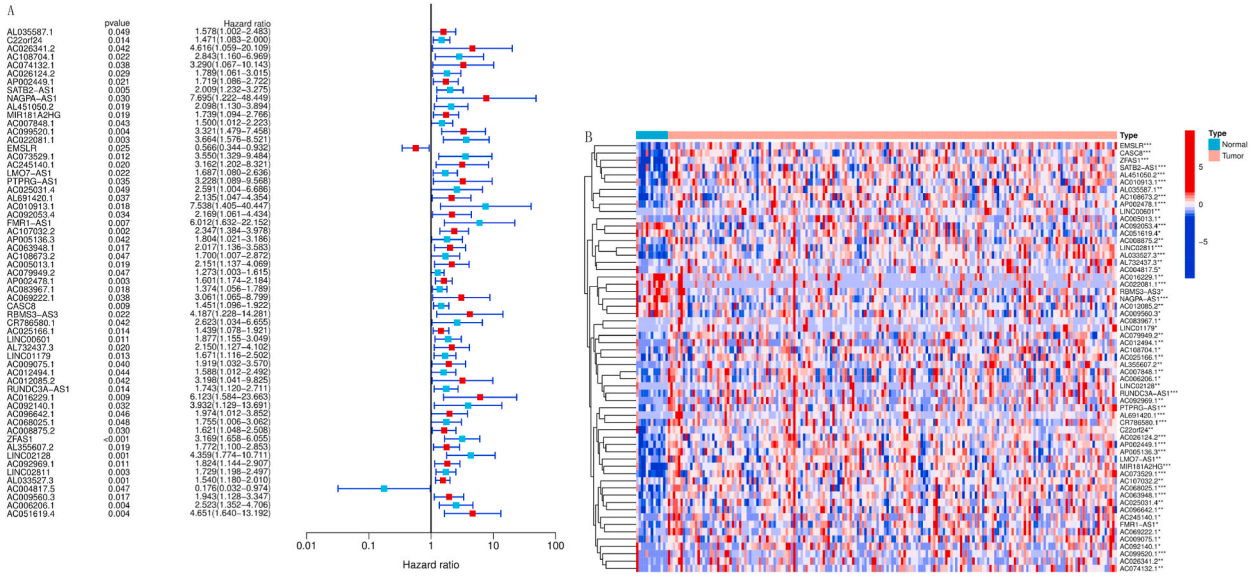

Fig. 2. Identification of the anoikis-related lncRNAs in esophageal cancer. (A) Forest plot of prognostic lncRNAs filtered by univariate Cox regression analysis; (B) Heatmap of prognostic lncRNAs expressed in the normal and tumor samples.

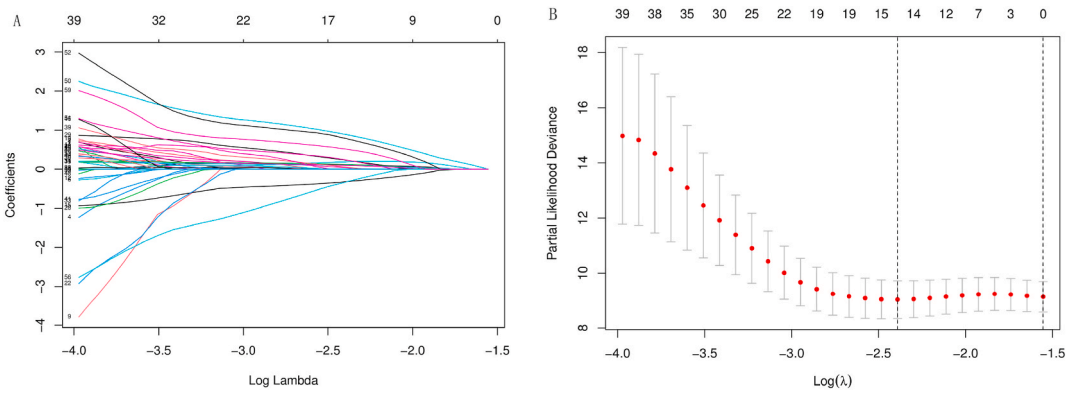

Fig. 3. Screening of prognostic anoikis-related lncRNAs by LASSO-Cox regression. (A) LASSO regression coefficients of the lncRNAs related to survival. (B) Cross-validation for optimal parameter selection to filter anoikis-related lncRNAs.

between the low-risk and high-risk groups. It demonstrated a distinct separation in outcome between the 2 groups ($P < 0.001$, Fig. 4A). Notably, the high-risk group exhibited a significantly inferior prognosis to the low-risk group. AUC was computed to evaluate the predictive performance of the risk score model. For the 1-year survival prediction, the AUC was 0.731, indicating favorable predictive accuracy. AUC values of 0.758 for 3-year and 0.784 for 5-year survival predictions confirmed the robustness of our risk signature (Fig. 4B). Additionally, the AUC of our risk score model was the largest in comparison with other clinical factors, with an AUC = 0.731 (Fig. 4C). To further validate the performance of our risk score model, we used the external GSE53622 dataset. In predicting the 1,3,5-year survival of the EC patients, the AUC of our risk score model was 0.735, 0.701, 0.776, respectively (Fig. 4D). Therefore, our risk score model performed well in evaluating the prognosis of EC patients.

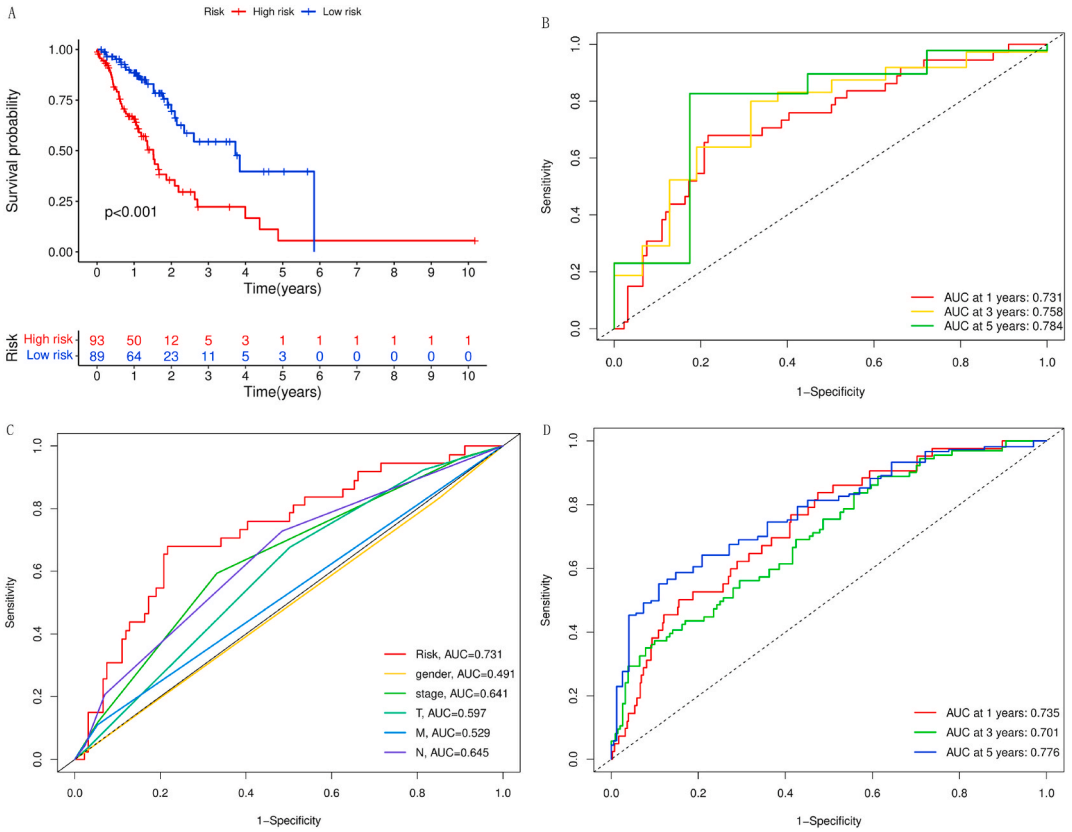

Fig. 4. Evaluate the risk score model. (A) Kaplan-Meier survival analysis of the EC patients in different risk groups. (B) ROC curves illustrating the predictive accuracy of the risk model in different survival time. (C) ROC curves of the risk model and other clinical factors, such as T-stage, N-stage and M-stage. (D) ROC curves for predicting the 1,3,5-year survival of the EC patients by risk score in the validation set.

3.4. Prognostic significance of the risk score model in EC

The distribution of EC patients based on their calculated risk scores is depicted. The ascending curve shows the distribution of samples along the risk score spectrum, highlighting the separation between low-risk and high-risk groups (Fig. 5A). This distribution underscores the model's ability to stratify patients according to their prognostic risk scores. Next, we analyzed the relationship between risk score and the vital status of each patient. In this scatter plot, more patients in the low-risk group are represented in blue and are clustered to the left of the dotted line, while more patients in the high-risk group are depicted in red and are clustered to the right of the dotted line (Fig. 5B). This visual representation underscores the correlation between higher risk scores and adverse survival outcomes. The expression pattern of anoikis-related lncRNAs within the risk model was analyzed. The heatmap visualizes the variations in the expression levels of these lncRNAs between different risk groups. For instance, *CASC8* and *ZFAS1* are upregulated in the high-risk group, while *AC004817.5* is downregulated in this group (Fig. 5C). For better visualization of the difference between the low

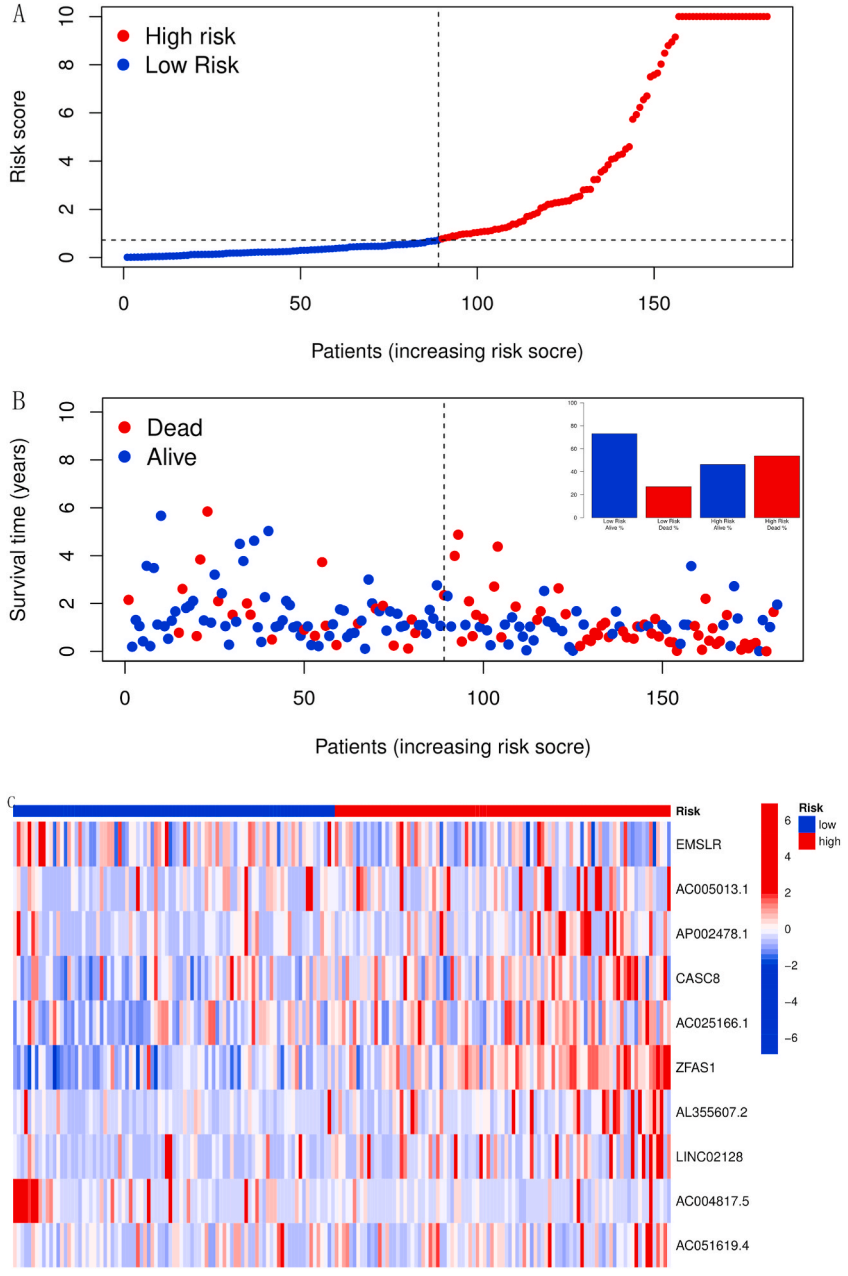

Fig. 5. Risk score analysis and prognostic insights. (A) Distribution of EC patients based on risk score. (B) The correlation between patients' risk score and survival outcomes. (C) Differential expression patterns of anoikis-related lncRNAs within the risk score model.

and high groups, we added boxplots of these lncRNAs to reveal the differential expression patterns (Supplementary Fig. S3). This examination of the risk score model's performance reflects its potential as a useful tool for prognosis evaluation of the EC patients.

3.5. Subgroup survival analysis

The impact of tumor stage on patient prognosis in EC is widely acknowledged. To further evaluate the prognostic value of our anoikis-related lncRNA signature, we conducted subgroup survival analysis based on tumor stage. We presented the KM plots for both early-stage (Stage I-II) and late-stage (Stage III-IV) EC patients. Interestingly, among the early-stage patients, there was no significant difference in OS between the low-risk and high-risk groups ($P > 0.05$, Fig. 6A). However, in the late-stage EC patients, a notable discrepancy in OS was observed between the low-risk and high-risk groups ($P < 0.05$, Fig. 6B). Importantly, the high-risk group displayed a significantly poorer survival, hinting the signature's potential to effectively distinguish risk categories among patients at a more advanced stage of EC. In addition, we further analyzed the lncRNA expression pattern between the low-risk and high-risk groups in different stage subgroups. In the early-stage patients, *AP002478.1, CASC8, AC025166.1, ZFAS1, AL355607.2* were significantly more expressed in the high-risk group ($P < 0.05$, Supplementary Figs. S2A and B). In the late-stage patients, *ZFAS1* was overexpressed in the high-risk group, while *AC004817.5* was overexpressed in the low-risk group ($P < 0.05$, Supplementary Figs. S2C and D). So these lncRNAs display different expression patterns in the stage subgroups. Among these ten lncRNAs, *AP002478.1, CASC8, AC025166.1, ZFAS1, AL355607.2* are more differential in the early stage, while *ZFAS1* and *AC004817.5* are more targeting the late stage EC patients.

3.6. Nomogram for predicting survival rate of EC patients

To improve the prognosis evaluation of EC patients, we integrated the anoikis-related lncRNA signature with clinical factors such as gender and tumor stage, and constructed a nomogram. This nomogram serves as a useful tool for predicting the survival rates of EC patients. For instance, consider a male patient in high risk group, with clinical characteristics like stage II, T2, M0, N0. When the scores of these attributes are combined, yielding a total score of 216 as determined by the nomogram, the prognostic predictions become tangible. Specifically, the nomogram anticipates a 1-year OS rate of 84.8 %, a 3-year OS rate of 33.6 %, and a 5-year OS rate of 4.33 % for this patient (Fig. 7). This nomogram can integrate risk score and clinical information into easily interpretable prognostic predictions for the EC patients.

3.7. Association between risk score and immune cell infiltration

We delved into the interplay between risk score and immune cell infiltration in the EC microenvironment, employing an array of algorithms including XCELL, TIMER, QUANTISEQ, MCP-counter, EPIC, CIBERSORT, and CIBERSORTABS (Fig. 8A). Our analysis focused on the Spearman correlation between patients' risk score and the abundance of infiltrating immune cells. Significant correlations between the risk score and specific immune cell populations came to light. Notably, eosinophils and common lymphoid progenitors demonstrated a positive association with the risk score ($R > 0$). This significant relationship was accentuated by the upward trajectory of the simulation line in the scatter plots (Fig. 8B and C). Conversely, a contrasting scenario unfolded for endothelial cells and myeloid dendritic cells, displaying negative correlations with the risk score ($R < 0$). This negative correlation was displayed by the downward trend of the simulation line in the scatter plots (Fig. 8D and E). These findings indicate the intricate landscape of immune cell infiltration influenced by the risk score, unraveling potential roles of distinct immune cell subsets in the EC microenvironment.

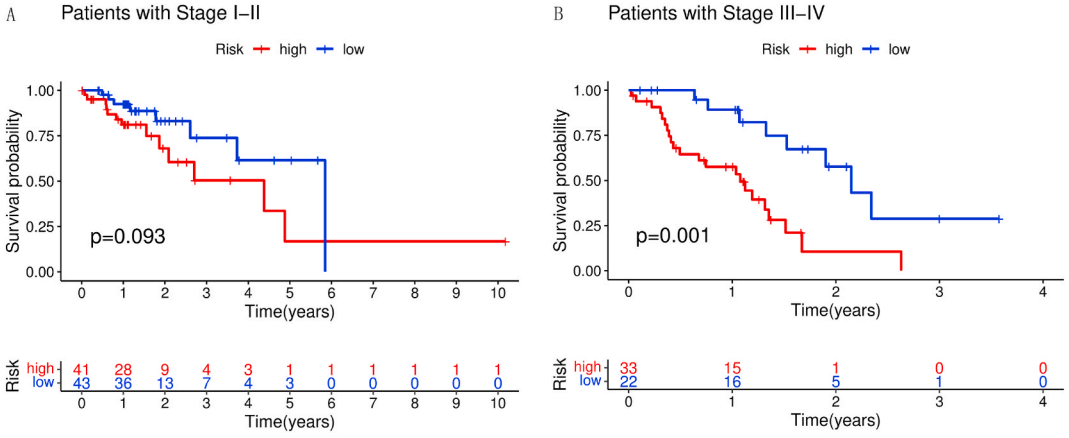

Fig. 6. Stratified survival analysis of the EC patients based on tumor stage. (A) Kaplan-Meier plot of the early stage EC patients (Stage I-II). (B) Kaplan-Meier plot of the late stage EC patients (Stage III-IV).

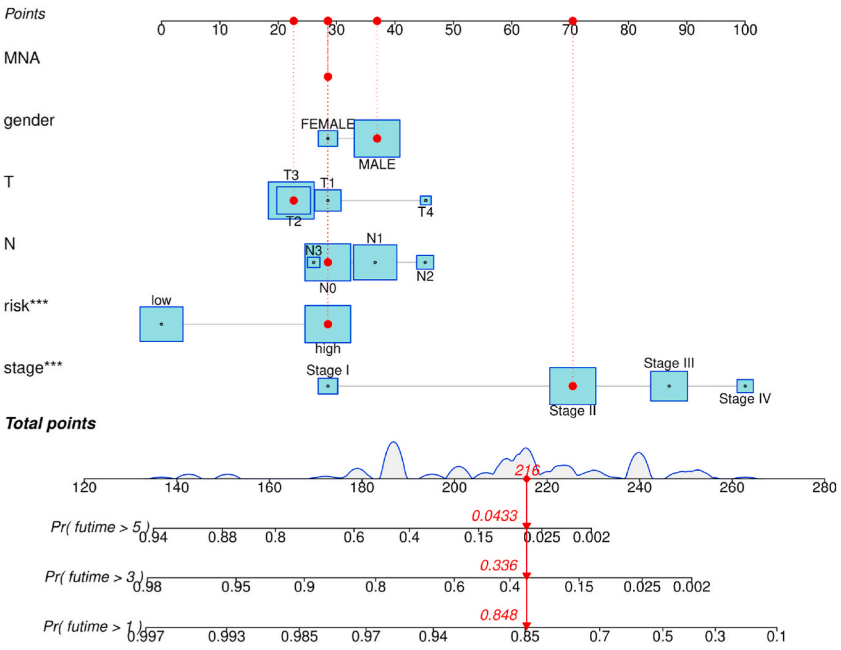

Fig. 7. Nomogram for predicting the 1-, 3-, and 5-year overall survival of the patients.

3.8. Association between risk score and drug sensitivity

We explored the interplay between risk score and drug sensitivity with the oncoPredict tool, assessing the potential of risk score as a predictive marker for therapeutic response. A distinct trend emerged through these analyses, elucidating some sensitive drugs for the patients in different risk groups. Concretely, a cluster of drugs, including ZM447439 (Fig. 9A), GSK269962A (Fig. 9B), KU-55933 (Fig. 9C), Osimertinib (Fig. 9D), Savolitinib (Fig. 9E), and Uprosertib (Fig. 9F), exhibited lower IC50 values in the low risk group. This finding reflects the potential of enhanced drug sensitivity for EC patients in the low risk group. Overall, our analysis reveals a significant correlation between the anoikis-related lncRNA signature and drug sensitivity, particularly to a range of small molecular drugs.

4. Discussion

EC is known for heterogeneous immune landscape, diverse clinical outcomes and intricate underlying mechanisms [13], our study has explored the role of anoikis-related lncRNAs, revealing their potential as molecular arbiters in the pathogenesis and prognosis of EC. Central to our findings is a risk score model derived from the expression profile of ten prognostic lncRNAs, poised to refine patient stratification and prognostication. Moreover, our study delved into the interactions between the risk score and immune cell infiltration as well as drug sensitivity. Generally, these findings provide an insight on the interplay of molecular signatures, immune responses, and therapeutic options in EC.

The construction of predictive models that incorporate molecular signatures has emerged as a potent approach to enhance prognostic assessment in various cancers [14]. In our study, we established a novel risk score model hinging on a panel of ten prognostic anoikis-related lncRNAs. This signature was tailored to harness the unique contribution of each lncRNA to prognostic stratification [15]. Our risk score model successfully classified patients into distinct risk groups, delineating those at high risk of adverse outcomes. The validation of this model through external GSE53622 dataset further confirmed its predictive potency. The AUC values for 1-year, 3-year, and 5-year survival predictions further indicated the model's reliable predictive performance. Importantly, the risk score model's predictive accuracy exceeded that of traditional clinical factors. These results suggest that our anoikis-related lncRNA signature may enhance the prognostic evaluation beyond conventional clinical parameters [16]. The validation process strengthens our confidence of our risk signature as a useful prognostic tool for the EC patients.

To delve into the molecular underpinnings of our risk signature, we analyzed the expression pattern of the anoikis-related lncRNAs within the model. The differential expression pattern between two risk groups provides an insight into the association between specific lncRNAs and patient outcomes. Notably, the upregulation of lncRNAs, such as CASC8 and ZFAS1, was observed in the high-risk group. The lncRNA CASC8 has been reported to involve in the immune landscape in pancreatic cancer, and could predict the clinical prognosis of such patients [17]. The lncRNA ZFAS1/miR-642a-5p axis regulated the tumor progression and immune cell infiltration of colon adenocarcinoma [18]. This analysis underscores the potential of these specific lncRNAs as key contributors to the model's ability to distinguish between different risk groups. Manipulating these lncRNAs may be feasible for therapeutic purposes.

The clinical heterogeneity of EC necessitates the stratification of patient cohorts to gain a deeper insight into prognostic

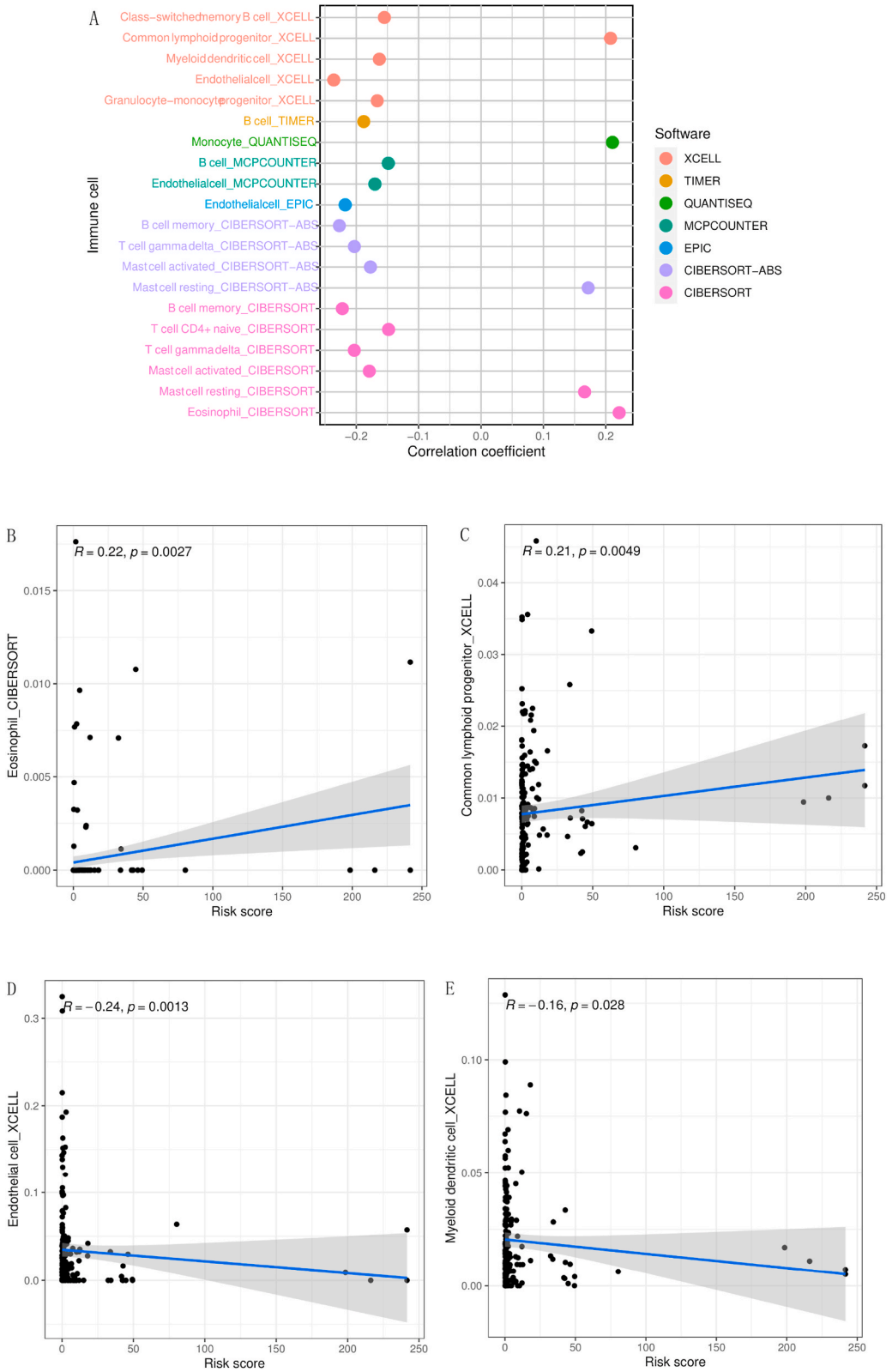

Fig. 8. Correlation between risk score and different immune cell infiltration. (A) Bubble chart for immune cell correlation analysis. (B) Eosinophil. (C) Common lymphoid progenitor. (D) Endothelial cell. (E) Myeloid dendritic cell.

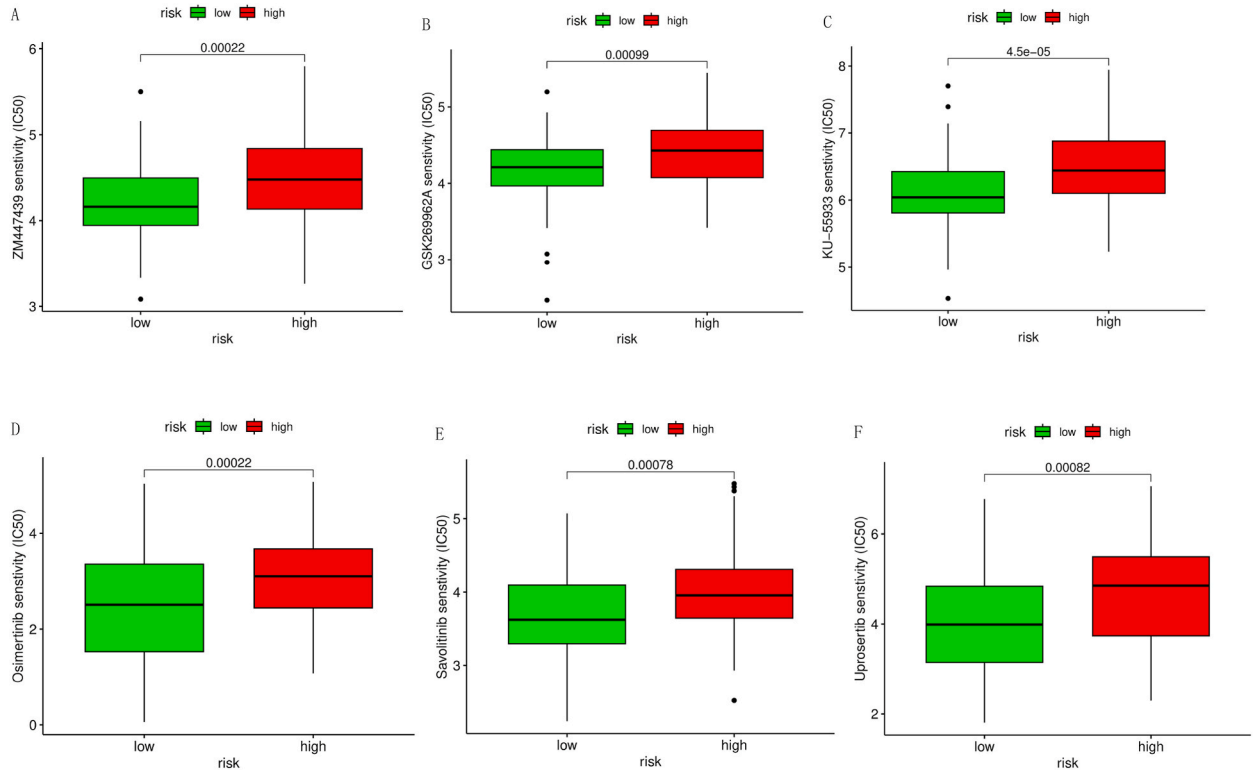

Fig. 9. Comparison of drug sensitivity between the low and high risk groups, including (A) ZM447439, (B) GSK269962A, (C) KU-55933, (D) Osimertinib, (E) Savolitinib, and (F) Uprosertib.

implications [19]. Our subgroup analysis based on tumor stage reaffirmed the discriminative power of our risk score model. The significant stratification in advanced-stage patients highlights the model's ability to distinguish prognosis, providing additional prognostic value beyond conventional clinical features. The integration of clinical factors with molecular signatures has the potential to refine prognostic assessments [20]. In our study, we introduced a nomogram that amalgamates clinical characteristics with the anoikis-related lncRNA risk score. This nomogram synthesizes clinical information into a tangible visual representation, enabling doctors to assess survival probabilities based on a combination of patient-specific variables [21]. This integrative approach provides a user-friendly tool for individualized prognosis evaluation.

We further examined the interplay between the risk score and immune cell infiltration in the EC microenvironment. Eosinophils and common lymphoid progenitors showed a positive correlation with the risk score. The measurement of eosinophil content in peripheral blood could serve as a promising indicator for reflecting the susceptibility to immune-related adverse events in patients undergoing treatment with PD-1/PD-L1 inhibitors, particularly in advanced malignancies [22]. In contrast, endothelial cells and myeloid dendritic cells displayed negative correlations with the risk score. Increased infiltration of endothelial cells was known to trigger the highest Autotaxin expression in the human breast cancer microenvironment, and mitigate tumor progression in early breast cancer [23]. Dendritic cells with capacity to initiate T cell activation fosters a potent anti-tumor immune response [24]. We appreciate the modest correlation coefficients observed between the risk score and immune cell infiltration. While these coefficients are $\pm$ 0.2, even weak correlations can yield some insights. Notably, the observed correlations were statistically significant and aligned with emerging research highlighting the nuanced roles of specific immune cells in EC [25]. We speculate that these correlations may contribute to a preliminary understanding of the immunological landscape in EC and warrant further investigation. Exploring the connection between the risk score and drug sensitivity unveiled intriguing results. Drugs such as ZM447439, GSK269962A, KU-55933, Osimertinib, Savolitinib, and Uprosertib exhibited enhanced sensitivity in the low-risk group. This observation reflects the value of our anoikis-related lncRNA signature as a tool for predicting drug responses in tailored treatment.

Some limitations should be concerned. First, the effects of potential confounding variables, such as differences in treatment modalities and patient comorbidities, have not been completely curbed, which may influence the prognostic implications of our model. Second, the intersection of immune infiltration and drug sensitivity with prognosis in our study also needs empirical substantiation, as the predictive value of these correlations has yet to be established in a clinical context. Third, functional roles of identified lncRNAs require experimental validation. Acknowledging these limitations, we advocate for longitudinal studies that chart the behavior of the lncRNAs in signature. Some of the selected ten lncRNAs seem to play different roles in the early-stage and late-stage patients, and that is what future longitudinal studies can focus on. Such longitudinal endeavors may illuminate the evolution of this risk score model in relation to disease progression and patient response to therapy. This aligns with the pivotal call for extended follow-ups, which could

reveal changes in molecular signatures and their prognostic significance over time.

5. Conclusion

This study has constructed an anoikis-related lncRNAs signature for assisting in the prognosis evaluation, immune infiltration assessment and treatment strategies in EC. Further investigations into the mechanistic roles of these lncRNAs, their potential as therapeutic targets, and their interactions with the immune microenvironment are likely to yield deeper insights, hopefully improving EC management and clinical outcomes.

Ethics approval and consent to participate

All procedures were in accordance with the ethical standards of the institutional research committee in Renmin Hospital of Wuhan University. We comply with the Helsinki declaration and its later amendments or comparable ethical standards.

Consent for publication

Not applicable.

Data availability statement

Data are available in the public, openly accessible TCGA and GEO database. All the data analysis results in this study are included in the manuscript and supplementary files.

Funding statement

This study is supported by the National Natural Science Foundation of China (82273094) and the Hubei Key Laboratory Opening Project (2021KFY064).

CRediT authorship contribution statement

Fan Feng: Writing – review & editing, Formal analysis. **Yuxin Chu:** Writing – original draft, Data curation. **Yi Yao:** Methodology. **Bin Xu:** Validation, Software. **Qibin Song:** Supervision.

Declaration of generative AI and AI-assisted technologies in the writing process

During the preparation of this work the authors used kimi.ai in order to improve language and readability. After using this tool service, the authors reviewed and edited the content as needed and take full responsibility for the content of the publication.

Declaration of competing interest

The authors declare that they have no known competing financial interests or personal relationships that could have appeared to influence the work reported in this paper.

Acknowledgements

The authors acknowledge the TCGA and GEO database for providing high-quality data for our study.

Appendix A. Supplementary data

Supplementary data to this article can be found online at https://doi.org/10.1016/j.heliyon.2024.e31202.

References

[1] A. Alotaibi, V.P. Gadekar, P.S. Gundla, S. Mandarthi, N. Jayendra, A. Tungekar, et al., Global comparative transcriptomes uncover novel and population-specific gene expression in esophageal squamous cell carcinoma, Infect Agent Cancer 18 (1) (2023) 47, https://doi.org/10.1186/s13027-023-00525-8.
[2] J. Ferlay, M. Colombet, I. Soerjomataram, C. Mathers, D.M. Parkin, M. Piñeros, et al., Estimating the global cancer incidence and mortality in 2018: GLOBOCAN sources and methods, Int. J. Cancer 144 (8) (2019) 1941–1953, https://doi.org/10.1002/ijc.31937.
[3] Y. Cheng, T. Chen, J. Hu, Genetic analysis of potential biomarkers and therapeutic targets in neuroinflammation from sporadic Creutzfeldt-Jakob disease, Sci. Rep. 13 (1) (2023) 14122, https://doi.org/10.1038/s41598-023-41066-9.

[4] T. Xin, Y. Sun, H. Meng, N. Zhang, B. Peng, X. Yang, et al., Identification of endoplasmic reticulum stress-related lncRNAs in lung adenocarcinoma by bioinformatics and experimental validation, Ann. Med. 55 (2) (2023) 2251500, https://doi.org/10.1080/07853890.2023.2251500.
[5] G. Hu, J. Li, Y. Zeng, L. Liu, Z. Yu, X. Qi, et al., The anoikis-related gene signature predicts survival accurately in colon adenocarcinoma, Sci. Rep. 13 (1) (2023) 13919, https://doi.org/10.1038/s41598-023-40907-x.
[6] L. Qiu, A. Tao, X. Sun, F. Liu, X. Ge, C. Li, Comprehensive bioinformatics analysis and experimental validation: an anoikis-related gene prognostic model for targeted drug development in head and neck squamous cell carcinoma, Oncol. Res. 31 (5) (2023) 715–752, https://doi.org/10.32604/or.2023.029443.
[7] D. Akca, A. Simon, R. Buettner, C. Bruns, W. Schroeder, T. Zander, et al., Syndecan-1 expression is an independent favourable prognostic marker in oesophageal adenocarcinoma and represents a potential therapeutic target, Oncol. Lett. 26 (2) (2023) 356, https://doi.org/10.3892/ol.2023.13942.
[8] Y. Jiang, Y. Ye, Y. Huang, Y. Wu, G. Wang, Z. Gui, et al., Identification and validation of a novel anoikis-related long non-coding RNA signature for pancreatic adenocarcinoma to predict the prognosis and immune response, J. Cancer Res. Clin. Oncol. (2023), https://doi.org/10.1007/s00432-023-05285-x.
[9] S. Du, K. Cao, Z. Wang, D. Lin, Comprehensive analysis of anoikis-related lncRNAs for predicting prognosis and response of immunotherapy in hepatocellular carcinoma, IET Syst. Biol. 17 (4) (2023) 198–211, https://doi.org/10.1049/syb2.12070.
[10] X. Diao, C. Guo, S. Li, Identification of a novel anoikis-related gene signature to predict prognosis and tumor microenvironment in lung adenocarcinoma, Thorac Cancer 14 (3) (2023) 320–330, https://doi.org/10.1111/1759-7714.14766.
[11] B. Chen, Y. Han, S. Sheng, J. Deng, E. Vasquez, V. Yau, et al., An angiogenesis-associated gene-based signature predicting prognosis and immunotherapy efficacy of head and neck squamous cell carcinoma patients, J. Cancer Res. Clin. Oncol. 150 (2) (2024) 91, https://doi.org/10.1007/s00432-024-05606-8.
[12] D. Maeser, R.F. Gruener, R.S. Huang, oncoPredict: an R package for predicting in vivo or cancer patient drug response and biomarkers from cell line screening data, Briefings Bioinf. 22 (6) (2021), https://doi.org/10.1093/bib/bbab260.
[13] J. Hippisley-Cox, W. Mei, R. Fitzgerald, C. Coupland, Development and validation of a novel risk prediction algorithm to estimate 10-year risk of oesophageal cancer in primary care: prospective cohort study and evaluation of performance against two other risk prediction models, Lancet Reg Health Eur 32 (2023) 100700, https://doi.org/10.1016/j.lanepe.2023.100700.
[14] X. Dong, P. Liao, X. Liu, Z. Yang, Y. Wang, W. Zhong, et al., Construction and validation of a reliable disulfidptosis-related LncRNAs signature of the subtype, prognostic, and immune landscape in colon cancer, Int. J. Mol. Sci. 24 (16) (2023), https://doi.org/10.3390/ijms241612915.
[15] Z. Tan, S. Fu, J. Zuo, J. Wang, H. Wang, Prognosis analysis and validation of lipid metabolism-associated lncRNAs and tumor immune microenvironment in bladder cancer, Aging (Albany NY) 15 (2023), https://doi.org/10.18632/aging.204975.
[16] L. Zhong, W. Qian, W. Gong, L. Zhu, J. Zhu, Development of anoikis-related long non-coding RNA signature associated with prognosis and immune landscape in cutaneous melanoma patients, Aging (Albany NY) 15 (15) (2023) 7655–7672, https://doi.org/10.18632/aging.204932.
[17] H. Ping, X. Jia, H. Ke, A novel ferroptosis-related lncRNAs signature predicts clinical prognosis and is associated with immune landscape in pancreatic cancer, Front. Genet. 13 (2022) 786689, https://doi.org/10.3389/fgene.2022.786689.
[18] B.X. Liu, J. Yang, C. Zeng, Y. Chen, MACC1 correlates with tumor progression and immune cell infiltration of colon adenocarcinoma and is regulated by the lncRNA ZFAS1/miR-642a-5p Axis, J Oncol 2022 (2022) 8179208, https://doi.org/10.1155/2022/8179208.
[19] Z. Yang, J. Gong, J. Li, H. Sun, Y. Pan, L. Zhao, The gap before real clinical application of imaging-based machine-learning and radiomic models for chemoradiation outcome prediction in esophageal cancer: a systematic review and meta-analysis, Int. J. Surg. 109 (8) (2023) 2451–2466, https://doi.org/10.1097/js9.0000000000000441.
[20] X. Shen, S. Wu, Z. Yang, C. Zhu, Establishment of an endoplasmic reticulum stress-associated lncRNAs model to predict prognosis and immunological characteristics in hepatocellular carcinoma, PLoS One 18 (8) (2023) e0287724, https://doi.org/10.1371/journal.pone.0287724.
[21] B. Zhao, W. Wu, L. Liang, X. Cai, Y. Chen, W. Tang, Prediction model of clinical prognosis and immunotherapy efficacy of gastric cancer based on level of expression of cuproptosis-related genes, Heliyon 9 (8) (2023) e19035, https://doi.org/10.1016/j.heliyon.2023.e19035.
[22] Y. Ma, X. Ma, J. Wang, S. Wu, J. Wang, B. Cao, Absolute eosinophil count may be an optimal peripheral blood marker to identify the risk of immune-related adverse events in advanced malignant tumors treated with PD-1/PD-L1 inhibitors: a retrospective analysis, World J. Surg. Oncol. 20 (1) (2022) 242, https://doi.org/10.1186/s12957-022-02695-y.
[23] M.G. Benesch, R. Wu, X. Tang, D.N. Brindley, T. Ishikawa, K. Takabe, Autotaxin production in the human breast cancer tumor microenvironment mitigates tumor progression in early breast cancers, Am. J. Cancer Res. 13 (7) (2023) 2790–2813.
[24] M. Dong, G. Zhang, J. Meng, B. Liu, D. Jiang, F. Liu, MMP9-Associated tumor stem cells, CCL1-silenced dendritic cells, and cytokine-induced killer cells have a remarkable therapeutic efficacy for acute myeloid leukemia by activating T cells, Stem Cells Int. 2023 (2023) 2490943, https://doi.org/10.1155/2023/2490943.
[25] Y. Chen, H. Zhou, Z. Wang, Z. Huang, J. Wang, M. Zheng, et al., Integrated analysis of ceRNA network and tumor-infiltrating immune cells in esophageal cancer, Biosci. Rep. 41 (5) (2021), https://doi.org/10.1042/bsr20203804.